

Dense arrays of Ge nanoclusters induced by low-energy ion-beam assisted deposition on SiO₂ films

A.V Dvurechenskii¹, P.L. Novikov¹, Y. Khang², Zh.V. Smagina¹, V.A. Armbrister¹, V.G. Kesler¹,
A.K. Gutakovskii¹

1. *Institute of Semiconductor Physics, Russian Academy of Sciences, Novosibirsk, Russia, dvurech@isp.nsc.ru*
2. *Samsung Electronics Co, Samsung Advanced Institute of Technology, Yongin-Si, Korea*

ABSTRACT

Ge islands less than 10 nm in base diameter and with a number density of about $8 \times 10^{11} \text{ cm}^{-2}$ were created on SiO₂ films by low-energy ion-beam assisted deposition in high vacuum. The structures obtained were analyzed by Electron Spectroscopy for Chemical Analysis, Atomic Force Microscopy and High Resolution Electron Microscopy. It was found that due to desorption at 300-375 °C less than 50% of Ge deposited remains at the surface. Only pulse regime of ion-beam action results in formation of nanoclusters. It is suggested that the simultaneous nucleation of Ge islands at pulse ion-beam action is the main reason of high homogeneity of size distribution of Ge nanoislands.

Keywords: semiconductor nanoparticles, ion-beam assisted deposition, silicon dioxide, nonvolatile memories

1. INTRODUCTION

Recently, considerable attention has been focused on semiconductor nanoparticles embedded into the silicon dioxide (SiO₂) of a metal-insulator-semiconductor (MOS) structures for future high speed and low power consuming logic and memory devices¹⁻⁴. The use of floating gate composed of isolated dots reduces the problems of charge loss encountered in conventional Flash memories, allowing for thinner injection oxides and, hence, smaller operating voltages, better endurance, and faster write/erase speeds. Moreover, the performance and the success of such a memory structure strongly depend on (a) the process ability for making uniform and reproducible thin tunnel oxides and (b) the characteristics of islands (such as crystallinity, size, shape orientation, spatial distribution) that influence both the potential energy of trapped electrons and the Coulomb blockade energy, which prevents the injection and storage of additional electrons.

In the previous works^{5,6} pulsed low-energy ion-beam-assisted deposition (IBAD) was implemented to stimulate Ge nanocluster array formation on Si(111) and Si(100). It was shown that the ion-beam action causes an increase in nanocluster density and size homogeneity. The idea of using the ion-beam action is that each ion impact into the continuous film (a) produces a vacancy cluster and (b) displaces an atom out from the bulk to the surface of the film⁷. The first factor facilitates the nucleation, while the second one increases the number of mobile adatoms assisting the precipitation process. Ion energy should be low enough to avoid introducing defects into SiO₂ sublayer, but high enough as compared to that of thermal Ge atoms. Regime of pulsed ion-beam irradiation causes simultaneous nucleation, favorable for highly homogeneous nanocluster size distribution.

In the present work IBAD was used to control the formation of Ge nanoisland arrays on SiO₂. The properties of Ge on SiO₂ surfaces (adhesion, surface and bulk diffusion, chemical properties) differ significantly from that on Si. The goal of the present study is to reveal and discuss the particularities of low-energy ion-beam action in these different conditions.

2. EXPERIMENTAL

The experiments were carried out in an ultrahigh-vacuum (UHV) chamber of molecular beam epitaxy setup equipped with effusion cell (boron nitride crucible) for Ge (Fig. 1). The system of ionization and acceleration of Ge⁺ ions provided the degree of ionization of Ge molecular beam from 0.1% to 0.5%. A pulse accelerating voltage supply unit generated ion-current pulses with duration of 0.5-1 s and ion energy of 50-200 eV. The angle of incidence of the molecular and ion

beams on the substrate was 54° to surface normal. The analytical section of the chamber included a reflection high-energy (20 keV) electron diffraction (RHEED) unit.

Prior to the deposition, the subsurface SiO_2 layer of 800 Å thick was formed by thermal oxidation of $\text{Si}(100)$ (60 min at 1000 °C in dry oxygen). After dioxide formation the wafers were washed in boiling $\text{C}_6\text{H}_5\text{CH}_3:\text{CH}_3\text{COCH}_3$ 1:10 and in boiling $\text{C}_6\text{H}_5\text{CH}_3:(\text{CH}_3)_2\text{CHOH}$ 1:5 solutions. Si/SiO_2 wafer was inserted into the ultrahigh-vacuum chamber. After heating the wafer up to 350-500 °C Ge deposition started. 3 monolayers (ML) of Ge were deposited without ion-beam irradiation. The rate of Ge deposition varied from 0.05 to 0.1 ML per second. After the deposition of 3 ML pulse ion-beam irradiation was applied at the effective Ge layer thickness 3 ML, 4 ML and 5 ML. It should be noted, that due to desorption the real Ge layer thickness was less than the effective one expected from the amount of Ge deposited. After the deposition of 5 ML the further Ge growth up to 20 ML was carried out without ion-beam action. Then the deposition was stopped, wafer cooled and extracted out from chamber. Only pulsed regime of ion-beam irradiation was used to avoid accumulating a static charge in the substrate. In the further description these conditions of preparation are assumed if they are not specified.

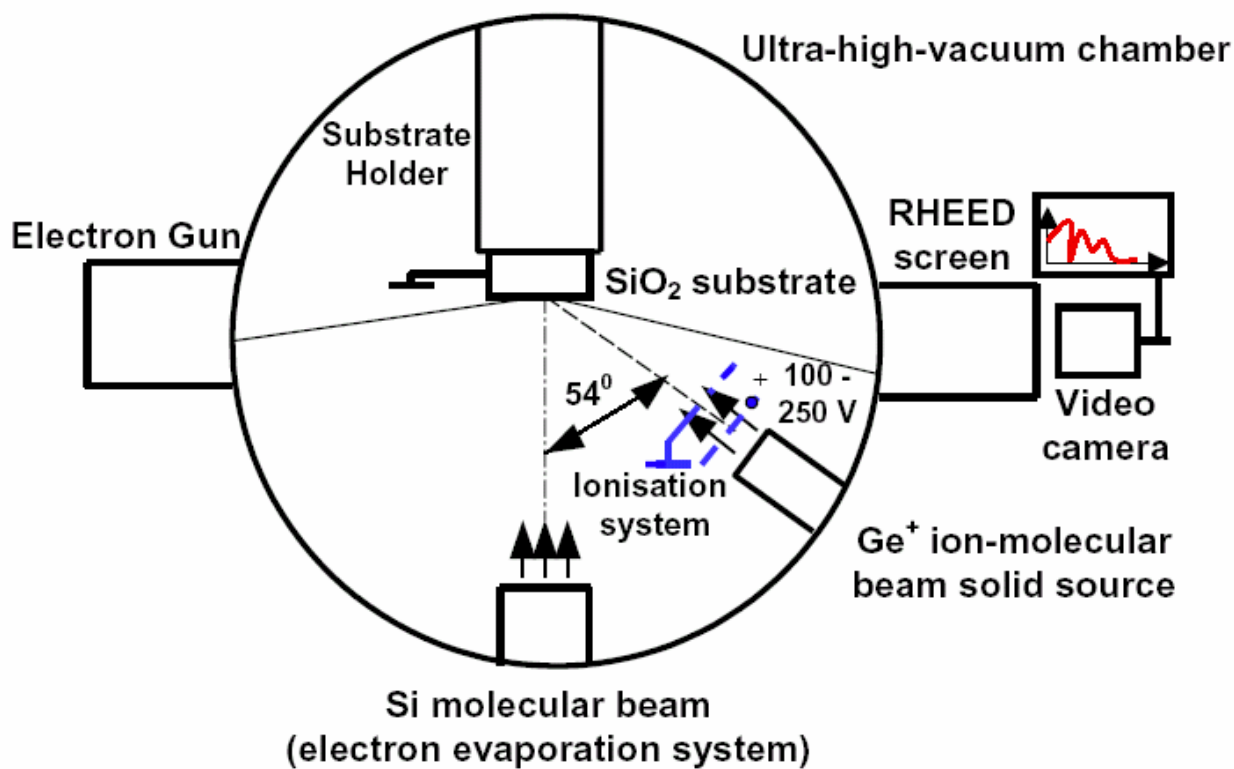


Fig. 1. MBE system with ion-beam source.

The structures grown by IBAD were analyzed by Electron Spectroscopy for Chemical Analysis (ESCA), Atomic Force Microscopy (AFM) and High Resolution Electron Microscopy (HREM).

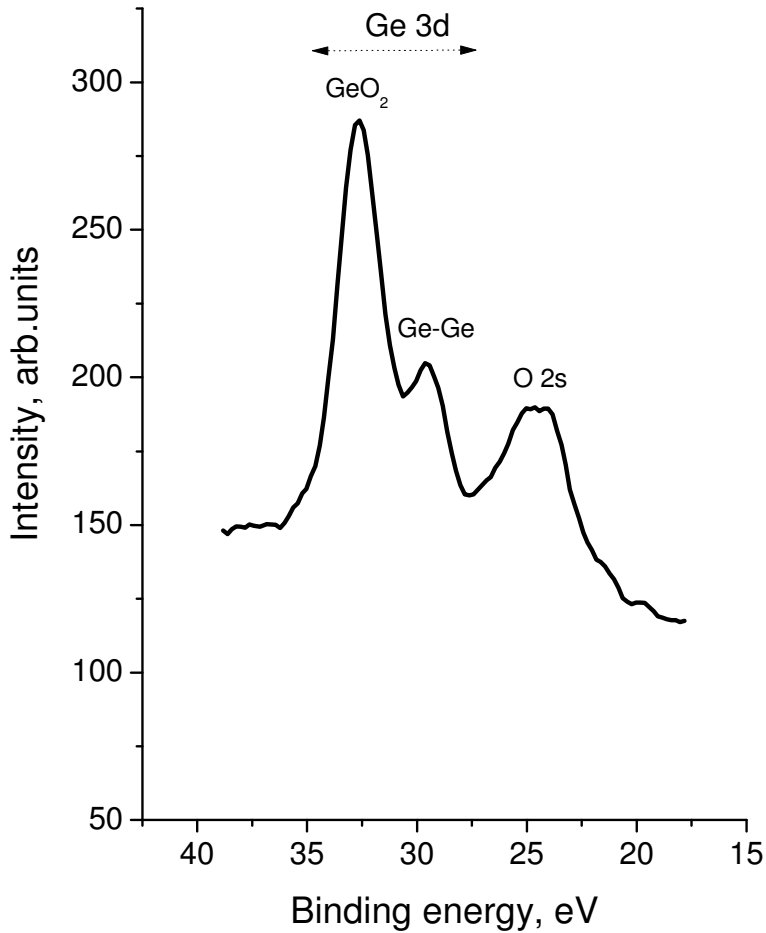


Fig. 2. ESCA spectrum from nc-Ge on SiO₂, grown by IBAD. The structure was prepared at 350 °C, Ge⁺ energy was 200 eV, pulses were applied at effective Ge layer thickness 3 ML, 4 ML and 5 ML. The amount of Ge deposited was 20 ML. Peak at 29 eV gives evidence of Ge content on the surface of the sample.

3. RESULTS AND DISCUSSION

3.1 Electron Spectroscopy for Chemical Analysis

In order to get information on chemical content of the surface, the samples after taking out from UHV chamber were analyzed by ESCA. The analysis was performed using SSC (RIBER, France). Al source with K α line 1486.6 eV was used for exciting X-ray Photoelectron spectra. The source power was 300 Watt, and X-ray beam diameter was 4-5 mm. The resolution of analyzer ΔE was 0.7 eV and the depth of probing was 1-4 nm. Fig. 2 presents the ESCA spectrum from nc-Ge on SiO₂ grown by IBAD. The structure was prepared at 350 °C, using pulse ion-beam irradiation with Ge⁺ energy 200 eV. The amount of Ge deposited was 20 ML. Two well defined peaks indicate the Ge content at the surface. The main peak at energy 32.6 eV and a smaller peak at 29.5 eV correspond to Ge2p (GeO₂) and Ge-Ge (Ge) respectively. The thickness of a layer, containing Ge, is estimated as 1.0 nm. These results give an evidence that at the deposition temperature an intensive oxidation and desorption of Ge take place. The mechanism of desorption is not

established yet. Apparently, due to interaction between germanium and oxygen, GeO composition is formed, which is weakly bonded to SiO₂ matrix. The desorption may proceed in the form of GeO (in this case the destruction of SiO₂ layer should also occur). Either, the decomposition reaction $2\text{GeO} \rightarrow \text{Ge} + \text{GeO}_2$ followed by Ge desorption may take place⁸. Ge content was also observed *in situ* by RHEED, which detected polycrystal phase with lattice parameter inherent to Ge.

ESCA gives no data on Ge nanocluster content in the surface. In order to define the morphology and microstructure of Ge layer, the samples were studied by AFM.

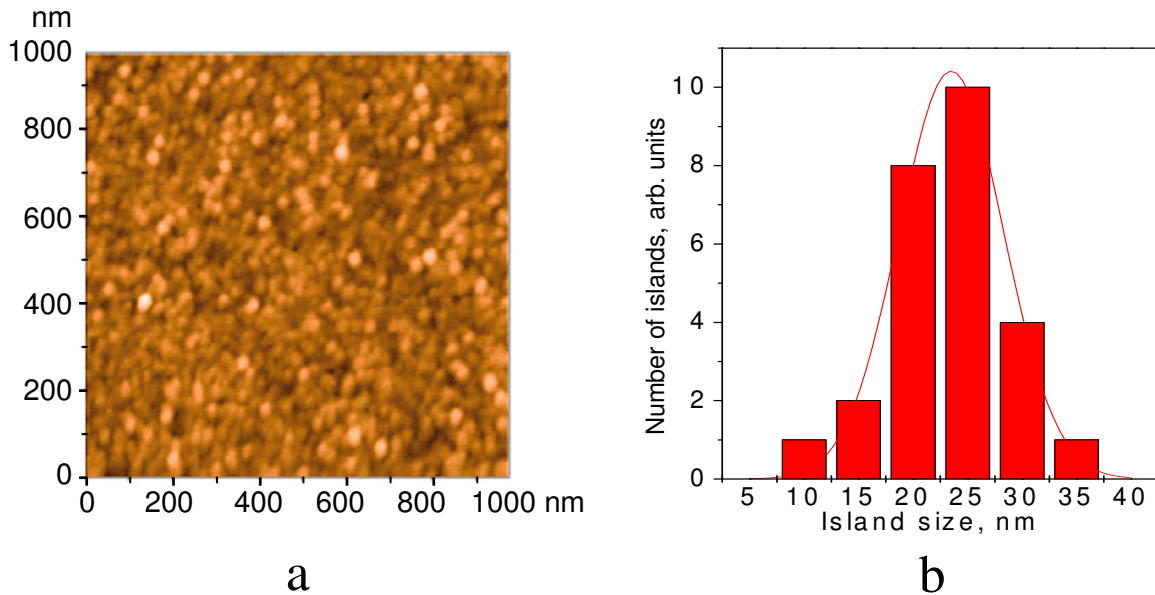


Fig. 3. a: AFM 100nm×100nm image of sample prepared by deposition of 20 ML of Ge at 350 °C on SiO₂ layer of 80 nm thick. 200 eV Ge⁺ pulses were applied at effective Ge layer thicknesses 3 ML, 4 ML and 5 ML; b: islands size distribution.

3.2 Atomic force microscopy

An AFM pattern observed for structures with 20 ML of Ge grown on SiO₂ by IBAD at 350 °C is shown in Fig. 3. The nanocluster structure is clearly defined in the image. An average size of islands is 28 nm, their deviation (size inhomogeneity) is 7.6 nm, island density is $7 \times 10^{10} \text{ cm}^{-2}$. Aspect ratio is approximately 25%.

An AFM pattern observed for structures with 16 ML of Ge deposited on SiO₂ at other conditions being equal is shown in Fig. 4. An average size of islands is 15 nm, their deviation is 4.5 nm, island density is $2 \times 10^{11} \text{ cm}^{-2}$.

One can expect, that the island number density is the parameter, which is predetermined at the initial stage of island formation, when nucleation occurs. However, the difference between the island number densities presented in Figs. 3, 4, respectively, indicates the more complicated mechanism of island evolution. Specifically, once being formed a cluster may disappear due to desorption or coalescence. It is also known, that at certain conditions ion-beam action may lead to so called inverse Ostwald ripening (IOR) phenomena, providing the mechanism of self-organization⁹. Since the degree of ionization of molecular beam is negligible, IOR is unlikely to be revealed in our experiments. However, at proper choice of experimental conditions IOR could be a promising tool of control a self-ordering process under IBAD.

The experiments were performed *ex situ*. That means the wafer with Ge layer deposited was transported to AFM via ambient atmosphere. The oxidation of Ge islands during transportation usually takes place. To check it and to carry out

the measurements of Ge island size excluding oxidation, some samples before taking out from UHV chamber were covered with Si cap layer and then studied by HREM.

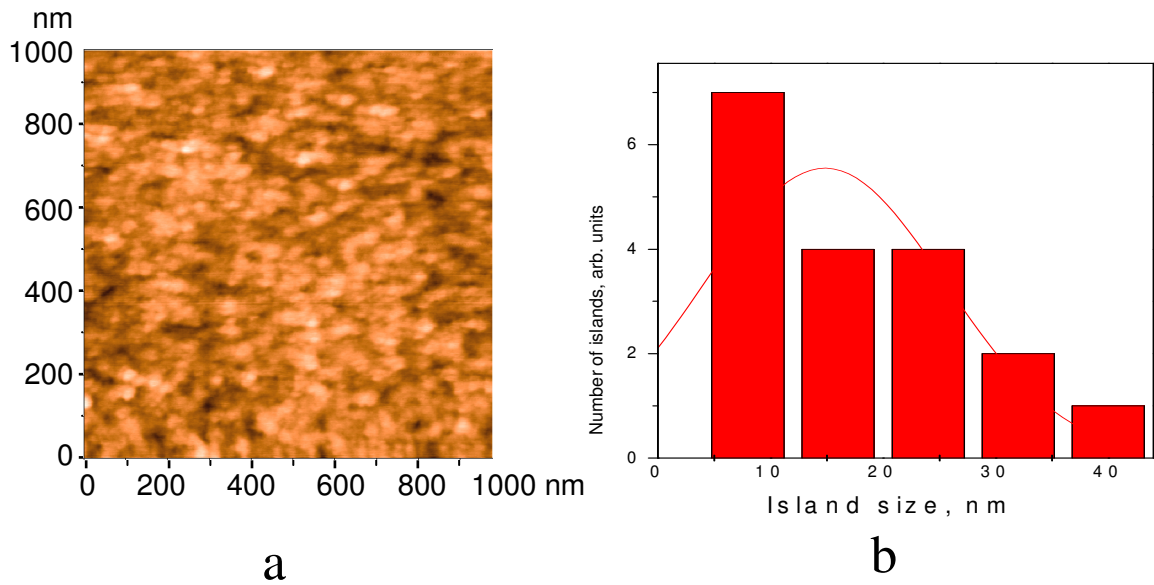


Fig. 4. a: AFM image of Ge-nc layer grown on SiO₂ by IBAD of 16 Ge ML; b: islands size distribution.

3.3 High resolution electron microscopy

HREM was performed using JEM-4000EX with resolution 0,17 nm at accelerating voltage 200 keV. HREM of two parts of a wafer was carried out. One part of wafer with Ge islands was capped by Si film at T=350 °C; another was uncapped (similar to AFM experiments). Both parts contained Ge layer formed by 20 ML Ge IBAD. HREM image shown in Fig. 5 presents the result for the capped nanocluster Ge layer prepared at the same conditions as that presented in Fig. 3. For the

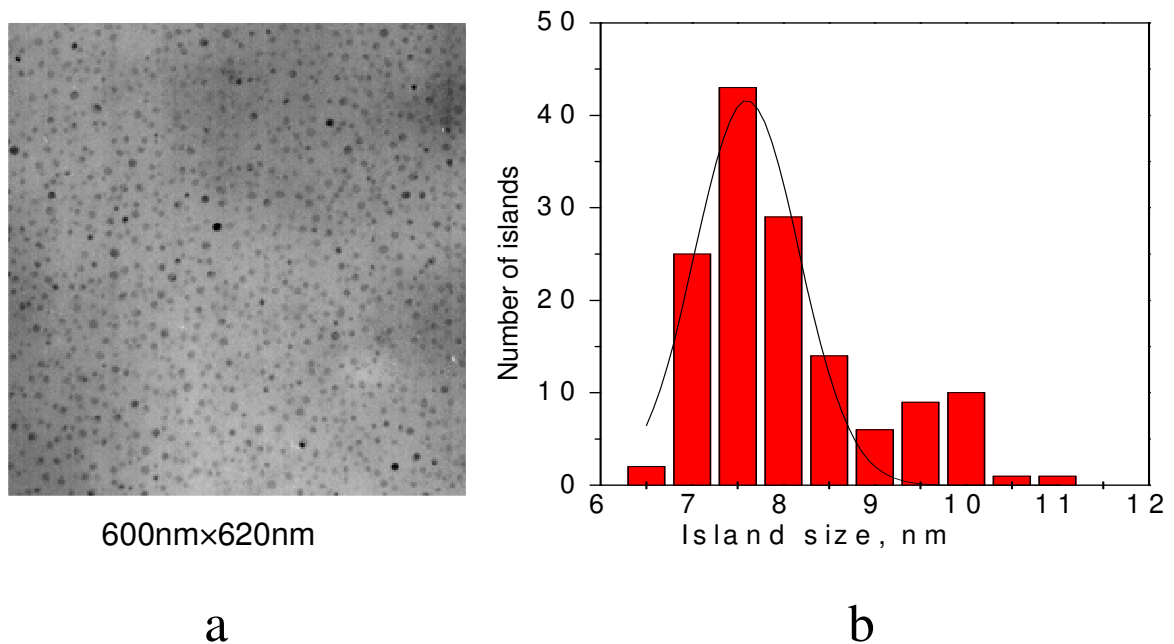
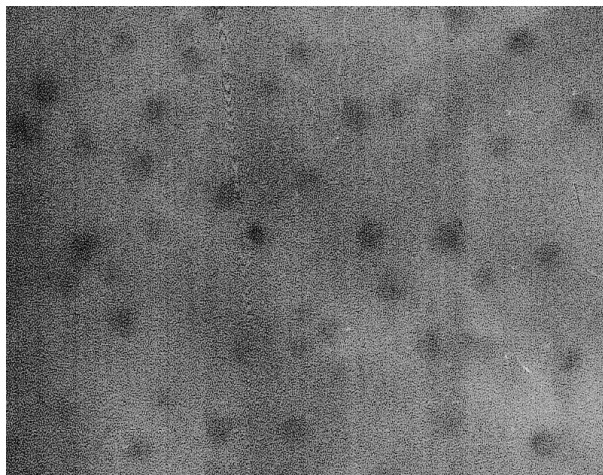
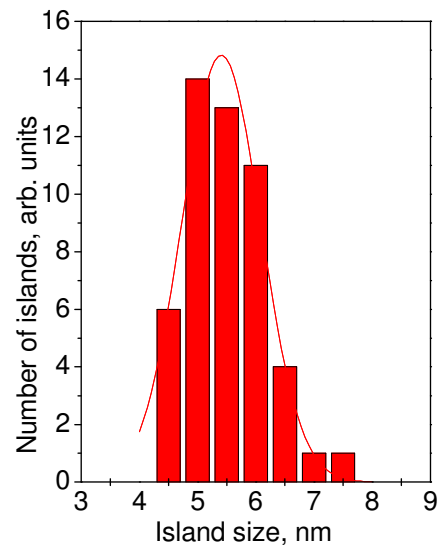


Fig. 5. a: HREM 600nm×620nm image of the sample prepared at the same conditions, as that shown in Fig. 3. Before HREM study, the sample was covered by a cap Si layer of 20 nm thick, preventing the Ge layer from oxidation at an ambient atmosphere; b: islands size distribution.



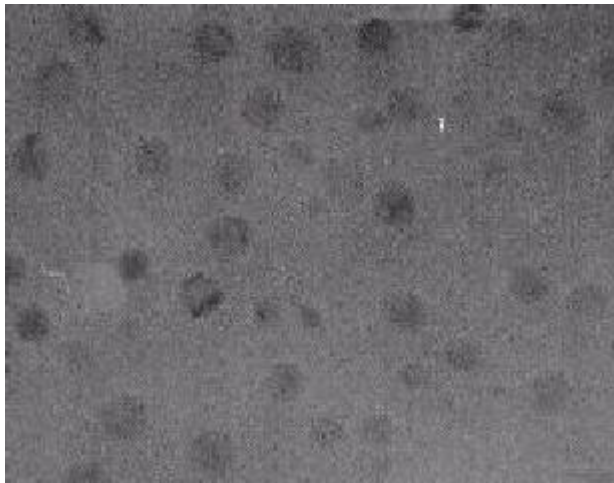
120nm×100nm

a



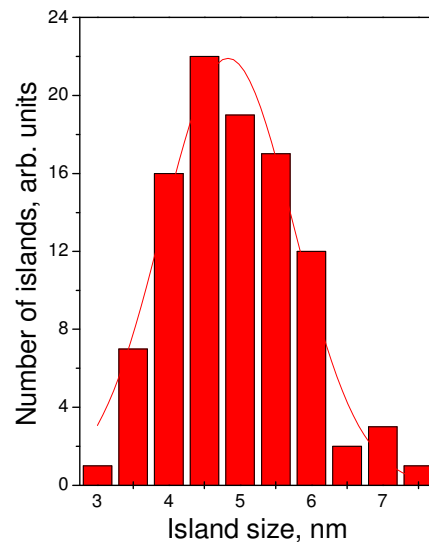
b

Fig. 6. a: HREM 120nm×100nm image of sample prepared by deposition of 20 ML of Ge at 300 °C on SiO₂ layer of 80 nm thick. 200 eV. Ge⁺ pulses were applied at effective Ge layer thicknesses 3 ML, 4 ML and 5 ML. Si layer of 15 nm thick was deposited above Ge layer at 15 °C; b: islands size distribution.



100nm×80nm

a



b

Fig. 7. a: HREM 100nm×80nm image of sample prepared by deposition of 20 ML of Ge at 375 °C on SiO₂ layer of 4 nm thick. After the predeposition of 3 Ge ML, 200 eV Ge⁺ pulses were applied during the further deposition at effective Ge layer thicknesses 3 ML, 4 ML and 5 ML; b: island size distribution estimated from HREM is 5±1 nm and 5.5·10¹¹ cm⁻², respectively.

capped sample the island density is $7 \times 10^{10} \text{ cm}^{-2}$, reproducing the result obtained by AFM. However, the size of islands is $7.6 \pm 1.2 \text{ nm}$, much less than that measured by AFM. These experiment clearly shows that *ex situ* measurements lead to enlarged islands size due to Ge oxidation in ambient atmosphere.

Fig. 6 presents the HREM image obtained for the sample, which was prepared by deposition of 20 ML of Ge at $300 \text{ }^\circ\text{C}$ on SiO_2 layer of 80 nm thick. 200 eV Ge^+ pulses were applied at effective Ge layer thicknesses 3 ML, 4 ML and 5 ML. Si layer of 15 nm thick was deposited above Ge layer at $15 \text{ }^\circ\text{C}$. The nanocluster size and density estimated from HREM is $5.4 \pm 0.7 \text{ nm}$ and $4 \times 10^{11} \text{ cm}^{-2}$, respectively.

For uncapped parts of the wafers HREM gives smaller nanocluster size. This is attributed to effect of oxidation, since an oxidized area of nanoclusters is invisible in HREM images.

In addition to the experiments presented above, we have implemented the IBAD method for Ge nanoclusters growth on a thin (of a few nm thick) SiO_2 film. The results were expected to be worse than those obtained in the case of thick SiO_2 film, since the new factors are included in the process of growth (mainly, Si and Ge diffusion through dielectric and much more dramatic effect of ion-beam action on the structure and thickness of SiO_2 layer). However, deposition on

SiO_2 film of 4 nm thick at $375 \text{ }^\circ\text{C}$ with other conditions being equal to the previous ones resulted in high homogeneous and dense array of Ge nanoclusters. The HREM image of the capped sample prepared in this regime is shown in Fig. 7. As estimated from HREM, the nanocluster density is $5.5 \times 10^{11} \text{ cm}^{-2}$ and nanocluster size $5 \pm 1 \text{ nm}$. Thus, in the case of thin SiO_2 film substrate IBAD is also a fruitful method.

We have not observed any nanostructured features in non-IBAD samples obtained at $300\text{-}375 \text{ }^\circ\text{C}$.

4. CONCLUSION

Study of Ge nanocluster formation on SiO_2 by low-energy ion-beam-assisted deposition was carried out. Using pulse regime of ion irradiation at deposition temperatures $300\text{-}375 \text{ }^\circ\text{C}$ results in formation of dense and homogeneous arrays of Ge nanoclusters. It was found, that mass transport process is dominated by desorption. The mechanism of desorption is ascribed either to formation of GeO composition or to elemental Ge sublimation. AFM images indicate nanostructured pattern at the surface of Ge layer. The size of nanoclusters is found to be increased due to oxidation at an ambient atmosphere. High-density and homogeneous arrays of Ge nanoclusters were also grown by IBAD on SiO_2 films of a few nm thick. The facility of IBAD method can be heightened by use of self-organisation mechanism provided by inverse Ostwald ripening.

5. ACKNOWLEDGEMENTS

This investigation was supported by Russian Foundation for Basic Research (Project 05-02-16285-a).

REFERENCES

- ¹ S. Tiwary, , F. Rana, H. Hanafi, A. Harstein, E. Crabbé, and K. Chan, "A silicon nanocrystals based memory", *Appl. Phys. Lett.* **68**, pp. 1377-1379, 1996.
- ² A. Shklyayev, M. Shibata, and M. Ichikawa, "High-density ultrasmall epitaxial Ge islands on Si(111) surface with a SiO_2 coverage", *Phys. Rev. B* **62**, 1540-1543, 2000.
- ³ D.-W. Kim, S. Hwang, T.F. Edgar, and S. Banerjee, "Characterization of SiGe Quantum Dots on SiO_2 and HfO_2 Grown by Rapid Thermal Chemical Deposition for Nanoelectronic Devices", *J. Electrochem. Soc.* **150**, pp. G240-G243, 2003.
- ⁴ Q. Wan, T.H. Wang, W.L. Liu, C.L. Lin, "Ultra-high-density Ge quantum dots on dielectric prepared by high vacuum electron-beam evaporation", *J. Cryst. Growth* **249**, pp. 23-27, 2003.
- ⁵ A.V. Dvurechenskii, V.A. Zinoviyev, V.A. Markov, V.A. Kudryavtsev, "Surface reconstruction induced by low-energy ion-beam pulsed action during Si(111) molecular beam epitaxy", *Surf. Sci.* **425**, pp. 185-194, 1999.

⁶ A.V. Dvurechenskii et al., “Ge/Si Nanostructures with Quantum Dots Grown by Ion-Beam Assisted Heteroepitaxy”, in *Quantum Dots: Fundamentals, Applications, and Frontiers* (B.A. Joyce et al. (eds.), 2005 Springer, printed in the Netherlands), pp. 135-144, 2005.

⁷ R. Ditchfield and E. G. Seebauer, “Semiconductor surface diffusion: Effects of low-energy ion bombardment”, *Phys. Rev. B* **63**, pp. 1253171-1253179, 2001.

⁸ N.N. Ovsyuk, E.B. Gorokhov, V.V. Grishchenko, and A.P. Shebanin, “Low-frequency Raman scattering by small semiconductor particles”, *JETP Letters* **47**, pp. 298-302, 1988.

⁹ K.-H. Heinig, “Inverse Ostwald Ripening and Self-Organization of Nanoclusters due to Ion Irradiation”, *invited talk MRS 2000 Fall Meeting, Boston, USA, Mat. Res. Soc. Proc.*, vol. **647**.